Pure & Appl. Chem., Vol. 65, No. 5, pp. 907–912, 1993.
Printed in Great Britain.

Thermophysical properties of fluids from acoustic measurements

M.B. Ewing

Department of Chemistry, University College London, 20 Gordon Street, London WC1H 0AJ, U.K.

Abstract - The speed of sound u is a mechanical property of a fluid and is linked to thermodynamics by the isentropic compressibility. Very precise values of u can be obtained from measurements of the radial resonance frequencies of a spherical resonator. Virial coefficients (both acoustic and p, V, T), heat capacities, the gas constant R, and thermodynamic temperature T are among the thermophysical properties that may be studied using the speed of sound. In addition, analysis of the loss mechanisms, which are observed as the resonance half widths, gives various transport properties, especially the relaxation times for energy transfer between the various modes of motion of the gas molecules.

INTRODUCTION

The use of acoustic methods to study the properties of fluids has a long history. For example, the speed of sound was used to establish that argon was monatomic. The first period of intense activity (ref. 1) followed the development of the Pierce oscillator (ref. 2) and, similarly, the impact of modern electronics resulted in precise apparatus and their use over wide ranges of temperature and pressure (ref. 3 - 6). All this work was based on cylindrical cavities but, more recently, spherical resonators have been developed into highly precise experimental tools (ref. 7 - 11). Although the construction of a sphere is more difficult, the advantages include the sharpest possible resonance frequencies (a result of the favourable surface-to-volume ratio), an insensitivity to geometric imperfections, and solutions in closed form for various corrections. Currently, the theory (ref. 8 - 11) gives corrections for the thermal boundary layer (including corrections for the curvature of the surface), the elastic response of the cavity, bulk dissipation in the gas, openings in the resonator's wall, and the temperature jump effect. The radial modes are especially useful because they have no viscous boundary layer which otherwise would be an important loss mechanism. These factors combine to make spherical resonators unrivaled instruments for measurements on gases especially at low pressures.

The isentropic compressibility κ_S provides the thermodynamic link between the speed of sound u in a fluid and its equation of state

$$u^2 = (\partial p/\partial \rho)_S = 1/\rho\kappa_S \tag{1}$$

where ρ is the mass density. For a gas, it is convenient to expand u^2 as a series in the amount density $\rho_n = n/V$

$$u^2 = A_0 + A_1\rho_n + A_2\rho_n^2 + \cdots \tag{2}$$

which is the acoustic analogue of the virial equation of state

$$p/\rho_n RT = 1 + B\rho_n + C\rho_n^2 + \cdots. \tag{3}$$

The speed of sound is obtained from the experimental resonance frequencies f_{0n} and half widths g_{0n} of the radial modes using

$$\nu_{0n}(u/2\pi a) = (f_{0n} + ig_{0n}) - \sum_j(\Delta f + ig)_j \tag{4}$$

where ν_{0n} is an eigenvalue and a is the radius of the sphere. The summation represents a series of corrections that are treated as perturbations. Note that the speed is obtained as (u/a) so the coefficients of equation (2) determined in the analysis of an isotherm are (A_i/a^2) and not A_i.

THERMODYNAMIC PROPERTIES

Virial coefficients

The second acoustic virial coefficient is defined by

$$\beta_a = RTA_1/A_0 \tag{5}$$

which is related to the second (p, V, T) virial coefficient B by a second-order differential equation:

$$\beta_a = 2B + 2(\gamma^{pg} - 1)T(dB/dT) + \{(\gamma^{pg} - 1)^2/\gamma^{pg}\}T^2(d^2B/dT^2). \tag{6}$$

Here $\gamma^{pg} = C^{pg}_{p,m}/C^{pg}_{V,m}$, is the ratio of the perfect-gas heat capacities. The intermolecular potential energy U may be obtained from β_a by integration (ref. 12) and, subsequently, other properties such as B may be calculated from U. However, to assess the internal consistency and to allow a comparison between acoustic and (p, V, T) virial coefficients, it is usually easier to avoid the direct solution of equation (6) by assuming a functional form for B such as

$$B = c_1 + c_2 \exp(c_3/T) \tag{7}$$

which may be derived from the square-well potential .

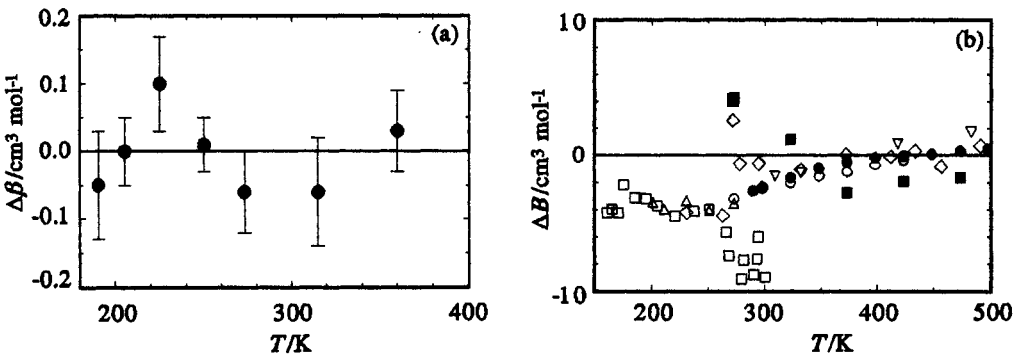

Fig. 1. Virial coefficients for Xe. (a) Deviations of β_a from equation (7): $\sigma(\beta_a) = 0.06$ cm^3 mol^{-1} or less than 0.05 per cent. The error bars are 1 standard deviation. (b) Deviations of other results from the acoustic measurements. ● ref. 14, ○ ref. 15, ■ ref. 16, □ ref. 17, △ ref. 18, ▽ ref. 19, ◇ ref. 20.

Figure 1(a) shows values of β_a for xenon (ref. 13) in the temperature range 190 to 360 K as deviations from equation (7): the results are internally consistent at the same level as the very small estimated errors in β_a. Deviations from literature values of B, which show considerable scatter, are plotted in Fig. 1(b) with a much less sensitive ordinate scale: all the results trend towards the same values at high temperatures. In a similar way, third acoustic virial coefficients γ_a, are obtained from A_2 but methods of obtaining estimates of the third (p, V, T) virial coefficient C from γ_a are less well established.

Properties from the limit of u^2 as $p \to 0$

The leading term of equation (2) is given by

$$A_0 = RT\gamma^{pg}/M. \tag{8}$$

Consequently, the speed of sound allows determination of γ^{pg}, and hence the heat capacities by a non-calorimetric method, the composition of a binary mixture through the molar mass M, and metrological measurements of the gas constant R and thermodynamic temperature T.

Heat capacities. Since (A_0/a^2) is the quantity obtained from analysis of an isotherm, the ratio of the heat capacities

$$\gamma^{pg} = (A_0/a^2)(M/RT)a^2 \tag{9}$$

requires the radius a. However, calibration measurements with a gas of known γ^{pg}, such as argon, gives

$$\gamma^{pg} = \tfrac{5}{3}\{M(A_0/a^2)\}/\{M(A_0/a^2)\}_{Ar} \tag{10}$$

and hence the perfect-gas heat capacity

$$C^{pg}_{p,m}/R = \gamma^{pg}/(\gamma^{pg} - 1) = \gamma^{pg}C^{pg}_{V,m}/R. \tag{11}$$

This procedure eliminates (a^2/RT) and, hopefully, some systematic errors in the experiment. Equation (11) implies that the fractional error in $C^{pg}_{p,m}$ will be a factor of $C^{pg}_{V,m}$ greater than that in (A_0/a^2) for the gas and the calibration. In practice, this level of accuracy is rarely achieved with hydrocarbons due to impurities and the consequent uncertainty in M. Figure 2(a) shows results for n-pentane and although the agreement with calorimetric and other work is satisfactory, the internal consistency is about a factor of 10 worse than might be hoped for.

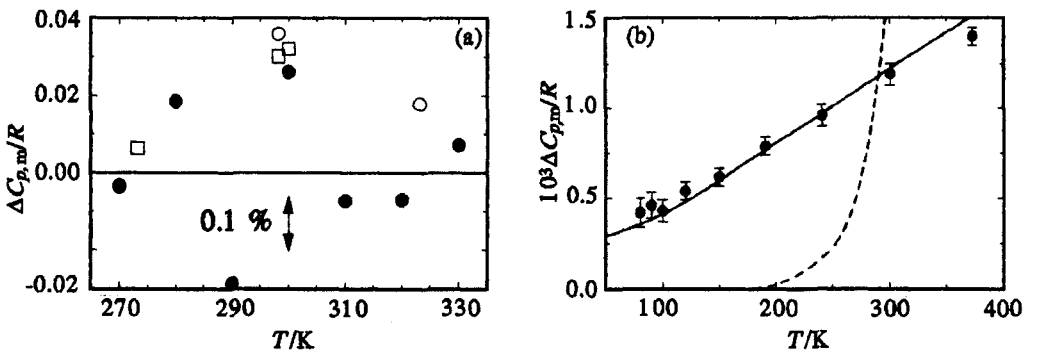

Fig. 2 Perfect-gas heat capacities (a) n-pentane ● deviations from the smoothing equation of ref. 22, ○ ref. 23, □ ref. 24. (b) $\Delta C^{pg}_{p,m} = C^{pg}_{p,m} - 3.5R$, for N_2 from ref. 25, —— including centrifugal distortion for rotation, – – vibrational contribution (not excited) .

Measurements with nitrogen between 80 and 373 K allowed a detailed test of acoustic determination of heat capacity. For nitrogen the characteristic temperatures for rotational and vibration are about 3 K and 3300 K, respectively. Consequently, it might be expected that rotation would be classical and vibration essentially unexcited; hence $C^{pg}_{p,m}$ should be $3.5R$. However, our experimental heat capacities exceed $3.5R$ by a small amount (always less than $0.0015R$) as Fig. 2(b) shows. The explanation is not, as one might think, the vibrational contribution, shown as the dashed curve in Fig. 2(b), because the experimental $C^{pg}_{p,m}$ are dynamic values obtained at frequencies well above the high-frequency limit for dispersion (the relaxation time $\tau \approx 1$ s for conversion between translation and vibration is very long for N_2). Rather the deviation of $C_{p,m}/R$ from 3.5 results from centrifugal distortion. The solid curve in Fig. 2(b) was calculated from statistical mechanics using spectroscopic values of the rotational constants and there is excellent agreement within our estimated experimental error of about $10^{-5}R$ except, perhaps, at the highest temperature where once again purity problems

are likely due to nervousness at degassing the resonator and its transducers at temperatures much above 373 K.

The gas constant and thermodynamic temperature. Measurements with a gas of known γ^{ps} and M at the temperature $T(H_2O, s+l+g)$ of the triple point of water (known exactly) provide a route to R. Acoustic determinations using cylinders (ref. 26) and spheres (ref. 10) have both been reported. In each case, the work probably represents the ultimate that can be achieved using current technology, but the work with a spherical resonator was more accurate by a factor of 5 demonstrating the superiority of spherical geometry at low pressures.

Again both cylinders (ref. 3) and spheres (ref. 27) have been used for primary acoustic thermometry with the necessary length measurements obtained from optical interferometry or dilatometry with mercury. However, the strong analogy that exists between acoustic and electromagnetic waves within a cavity permits an interesting alternative. An electromagnetic form of equation (4) may be written with the important difference that the speed of light c_0 in vacuum is defined exactly, so a measurement of the microwave resonance frequency f_c is equivalent to a measurement of the radius a. If the measurements are referenced to the temperature $T_r = T(H_2O, s+l+g)$ then

$$T/T_r = \{(A_0/a^2)_T / (A_0/a^2)_r\} \times (f_T/f_r)_c^2 + \cdots \tag{12}$$

where the microwave resonance frequencies f_c have been used in place of a and the $\cdots$ represent a series of corrections that must be made. So far we have applied this approach to temperatures over the range 100 to 373 K.

TRANSPORT PROPERTIES

The resonance half widths are the result of loss mechanisms which depend on transport properties such as thermal conductivity κ and viscosity η. To determine these quantities it is usually necessary to consider acoustic modes of different symmetry. In a sphere, for example, the viscous boundary is absent for radial modes but the non-radial modes have both thermal and viscous contributions. However, the design of a spherical resonator minimizes these effects and only rough estimates of κ and η can be obtained. Cylindrical resonators, with their much larger boundary layers, have been used to determine these quantities (ref. 3, 26).

An additional loss mechanism is possible for polyatomic molecules. The exchange of energy between the translational modes and the internal vibrational modes is often slow on a molecular time scale and may be characterized by a relaxation time τ. When the angular frequency $\omega = 2\pi f$ becomes comparable with $1/\tau$, the vibrational modes do not reach equilibrium during the acoustic cycle and the effective heat capacity is reduced

$$C_p(\omega) = C_p - \imath\omega\tau C_{vib}/(1 + \imath\omega\tau) \tag{13}$$

where C_{vib} is the vibrational contribution. Consequently, γ increases with frequency as does the observed speed. If a fraction $\Delta = C_{vib}/C_p$ of the total heat capacity relaxes with a time constant τ, then

$$\gamma(\omega)/\gamma \approx \omega\tau(\gamma - 1)\Delta\{\omega\tau(1 - \gamma\Delta) - \imath\} \tag{14}$$

from which it is clear that the imaginary part of $\{\gamma(\omega)\}^{1/2}$, which determines the contribution of vibrational relaxation to the half width g, is proportional to $\omega\tau$; whereas the speed dispersion, the real part of $\{\gamma(\omega)\}^{1/2}$, varies as $(\omega\tau)^2$. Consequently, provided $\omega\tau$ is small compared with unity (and equation 14 incorporates this assumption), estimates of τ can be made from the experimental half widths with sufficient accuracy for the difference $\{u(\omega = 0) - u(\omega)\}$ to be calculated with negligible error. If measurement of u is the principal objective, then the speed dispersion is merely another correction that must be made. However, these relaxation processes are a valuable source of

information for the transfer of energy within molecules and molecular collisions. Since the transfer is possible only during a collision (the number of which will be proportional to $1/\rho$), it is $\tau\rho$ (rather than τ alone) that is most nearly constant and (f/ρ) is the quantity one adjusts to sweep through a dispersion curve. Consequently, the capability of a spherical resonator to work at low pressures compensates to some extent for the low frequencies and there is good agreement between our values of $\tau\rho$ and those obtained at much higher frequencies (ref. 28).

MEASUREMENTS UNDER DIFFICULT CONDITIONS

Since the speed of sound is formally independent of the amount of substance, acoustic methods may be used to study the equation of state of a gas at low reduced temperatures where more conventional methods are often unreliable due to the effects of adsorption. A set of measurements for methanol illustrates the performance of the technique at low pressures. Figure 3(a) summarizes the results which cover the temperature range 280 to 360 K. For the lowest isotherm, the vapour pressure of methanol is only about 5 kPa and work was restricted to pressures below 3 kPa. These are rather unfavourable conditions since the correction for the thermal boundary layer reached 480×10^{-6} of $f_{0,2}$ for the first radial mode at a pressure of 1 kPa. Nevertheless, values of the speed of sound obtained from individual modes still agree to about 40×10^{-6} of u and the whole isotherm was internally consistent to about the same level. No doubt work could be extended to still lower pressures using appropriate transducers and signal averaging, but 1 kPa probably represents the practical limit of the experiment at this stage. However, it is not easy to visualize a (p, V, T) experiment with a relative precision of 10^{-5} for a polar fluid below 3 kPa.

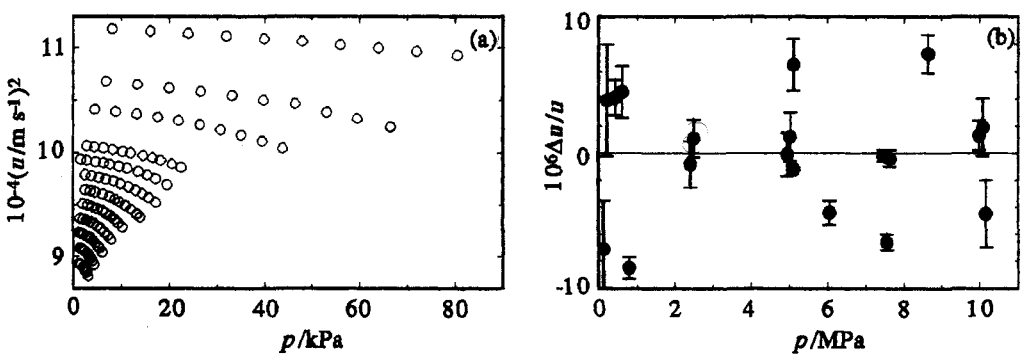

Fig. 3 (a) Isotherms between 280 and 360 K for methanol (ref. 29). (b) Deviations from a smoothing equation for $(0.85CH_4+0.15C_2H_6)$ at 300 K; the error bars are the standard deviation of $< u >$ at each pressure (ref. 30).

At high pressures the problems are rather different. The shell motion now dominates the corrections to the observed resonance frequencies and, at the highest pressure of the isotherm shown in Fig. 3(b) for the mixture $(0.85CH_4 + 0.15C_2H_6)$, the shell correction is about 10^{-4} of the observed frequency. Elastic anisotropy and minor shell resonances create problems, and considerable care must be exercised in selecting the appropriate modes for study. The deviations of the experimental results from a smoothing equation with 5 adjustable parameters are shown in Fig. 3(b) and we see that the agreement between modes at a particular pressure, and the consistency of the isotherm as a whole, is better than 10^{-5}. Since the shell correction is approximately linear in density, the performance of the experiment can be estimated at higher pressures. Thus an internal consistency of a few parts in 10^{-5} of u^2 should still be possible in a stainless steel resonator for argon at 20 MPa or methane at 50 MPa (densities of about 300 kg m^{-3}). However, other acoustic techniques, such as variable-path length cylinders and pulse methods, with their use of quartz transducers would be more appropriate, not least because the sample volume is smaller, as the density of liquids is approached.

Acknowledgements

I wish to acknowledge my collaborators: Drs. S.J. Boyes, A.R.H. Goodwin, J.C. Sanchez, and J.P.M. Trusler with whom the science has been profitable and fun. Dr. M.R. Moldover and Professor J.B. Mehl were the first to appreciate what could be done with spherical resonators and then set about doing it.

REFERENCES

1. J.C. Hubbard, Phys. Rev. 35, 1442-1443 (1926); 36, 1668-1669 (1930); 38, 1011-1019 (1931); 41, 523–525 (1932).
2. G.W. Pierce, Proc. Amer. Acad. 60, 269-302 (1925).
3. A.R. Colclough, Proc. R. Soc. Lond. A 365, 349-370 (1979).
4. B.E. Gammon and D.R. Douslin, J. Chem. Phys. 64, 203-218 (1976).
5. B.E. Gammon, J. Chem. Phys. 64, 2556-2568 (1976).
6. B.A. Younglove and R.D. McCarty, J. Chem. Thermodyn. 12, 1121-1128 (1980).
7. J.B. Mehl and M.R. Moldover, J. Chem. Phys. 74, 4062-4077 (1981).
8. M.R. Moldover, J.B. Mehl and M. Greenspan, J. Acoust. Soc. Amer. 79, 253-272 (1986).
9. M.B. Ewing, M.L. McGlashan and J.P.M. Trusler, Metrologia 22, 93-102 (1986).
10. M.R. Moldover, J.P.M. Trusler, T.J. Edwards, J.B. Mehl and R.S. Davies, J. Res. NBS 93, 85-144 (1988); Phys. Rev. Lett. 60, 249-252 (1988).
11. M.B. Ewing, A.R.H. Goodwin, M.L. McGlashan and J.P.M. Trusler, J. Chem. Thermodyn. 19, 721-739 (1987).
12. M.B. Ewing, M.L. McGlashan and J.P.M. Trusler, Mol. Phys. 60, 681-690 (1987).
13. S.J. Boyes, M.B. Ewing and U. Holländer, unpublished work.
14. J.A. Beattie, R.J. Barriault and J.S. Brierley, J. Chem. Phys. 19, 1219-1221 (1951); 19, 1222-1226 (1951).
15. A. Michels, T. Wassenaar and P. Louwerse, Physica 20, 99-106 (1954).
16. E. Whalley, Y.Lupien and W.G. Schneider, Can. J. Chem. 33, 633-636 (1955).
17. C.A. Pollard and G. Saville, quoted by Ref. 21.
18. R. Hahn, K. Schäfer and B. Schramm, Ber Bunsenges. Phys. Chem. 78, 287-289 (1974).
19. H.-P. Rentschler and B. Schramm, Ber Bunsenges. Phys. Chem. 81, 319-321 (1977).
20. B. Schramm, H. Schmeidel, R. Gehrmann, and R. Bartl, Ber Bunsenges. Phys. Chem. 81, 316-321 (1977).
21. J.H. Dymond and E.B. Smith, The virial coefficients of pure gases and mixtures, p. 251, Clarendon Press, Oxford (1980).
22. M.B. Ewing, A.R.H Goodwin and J.P.M. Trusler, J. Chem Thermodyn. 21, 867-877 (1989).
23. I.A. Hossenlopp and D.W. Scott, J. Chem Thermodyn. 13, 415-421 (1981).
24. D.W. Scott, J. Chem. Phys. 60, 3144-3165 (1974).
25. M.B. Ewing and J.P.M Trusler, Physica A184, 415-436 (1992).
26. A.R. Colclough, T.J. Quinn and T.D.R Chandler, Proc. R. Soc. Lond. A 368, 125-139 (1979).
27. M.R. Moldover and J.P.M. Trusler, Metrologia 25, 165-188 (1988).
28. M.B. Ewing and J.P.M. Trusler, J. Chem. Phys. 90, 1106-1115 (1989).
29. S.J. Boyes, M.B. Ewing and A.R.H. Goodwin, J. Chem Thermodyn. 24, 1151-1166 (1992).
30. S.J. Boyes, Ph.D thesis, Univ. Lond. (1992).